

Interfaces in polymer blends

Marcus Müller and Kurt Binder

Institut für Physik, WA 331, Johannes Gutenberg Universität
D-55099 Mainz, Germany
(IPC99, Yokohama, Macromolecular Symposia)

Summary: We investigate the structure and thermodynamics of interfaces in dense polymer blends using Monte Carlo (MC) simulations and self-consistent field (SCF) calculations. For structurally symmetric blends we find quantitative agreement between the MC simulations and the SCF calculations for excess quantities of the interface (e.g., interfacial tension or enrichment of copolymers at the interface). However, a quantitative comparison between profiles across the interface in the MC simulations and the SCF calculations has to take due account of capillary waves. While the profiles in the SCF calculations correspond to intrinsic profiles of a perfectly flat interface the local interfacial position fluctuates in the MC simulations. We test this concept by extensive Monte Carlo simulations and study the cross-over between “intrinsic” fluctuations which build up the local profile and capillary waves on long (lateral) length scales.

Properties of structurally asymmetric blends are exemplified by investigating polymers of different stiffness. At high incompatibilities the interfacial width is not much larger than the persistence length of the stiffer component. In this limit we find deviations from the predictions of the Gaussian chain model: while the Gaussian chain model yields an increase of the interfacial width upon increasing the persistence length, no such increase is found in the MC simulations. Using a partial enumeration technique, however, we can account for the details of the chain architecture on all length scales in the SCF calculations and achieve good agreement with the MC simulations.

In blends containing diblock copolymers we investigate the enrichment of copolymers at the interface and the concomitant reduction of the interfacial tension. At weak segregation the addition of copolymers leads to compatibilization. At high incompatibilities, the homopolymer-rich phase can accommodate only a small fraction of copolymer before the copolymer forms a lamellar phase. The analysis of interfacial fluctuations yields an estimate for the bending rigidity of the interface. The latter quantity is important for the formation of a polymeric microemulsion at intermediate segregation and the consequences for the phase diagram are discussed.

Introduction

Melt blending of polymers is a promising route for tailoring materials to specific application properties. Unlike metallic alloys, however, chemically different polymers often do not mix on microscopic length scales. Rather a complicated morphology of droplets of one component dispersed into the other component forms on a mesoscopic length scale, and the blend can be conceived as an assembly of interfaces. While the detailed structure on this mesoscopic length scale depends strongly on the way the material is processed, the local properties of interfaces are certainly crucial for understanding the material properties. The interfacial width sets the length scale on which entanglement between polymers of the different components form. Experiments¹ suggest that the mechanical strength in-

creases if the interfacial width exceeds the entanglement length. The interfacial tension is important for the breaking-up of droplets under shear^{2,3}: The lower the interfacial tension the finer dispersed the two components.

In the following we shall describe computer simulations in the framework of a coarse grained lattice model targeted at investigating the local structure of the interfaces between coexisting phases in polymer blends. The results are compared to self-consistent field calculations and a description via an effective interface Hamiltonian. In the next section we describe our computational model and the Monte Carlo technique. Then we detail our results on symmetric binary blends, binary blends of polymers with different stiffness, and a ternary blend of two homopolymers and a symmetric diblock copolymer. The paper closes with a short outlook.

Model and technique

The simulations are performed in the framework of the bond fluctuation model. In the framework of this coarse grained lattice model in three dimensions each monomer represents a small number of repeat units (say, 3-5) along the backbone of a polymer. Only the relevant interactions – excluded volume, connectivity, and a repulsion between unlike species – are retained. Each monomer blocks 8 corners of a unit cell of the simple cubic lattice from further occupancy. We work at a number density of $\rho = 1/16$. At this density the model reproduces many features of a dense melt, e.g., the screening of the excluded volume, but still allows for a fast relaxation of the chain conformations. Monomers are connected via one of 108 bond vectors of length $2, \sqrt{5}, \sqrt{6}, 3$, and $\sqrt{10}$ in units of the lattice spacing. The large number of bond vectors permits 87 distinct bond angles and yields a good approximation of continuous space. The bending stiffness of a polymer can be tuned by imposing a bending potential $E(\Theta) = f \cos(\Theta)$, where Θ denotes the angle between successive bond vectors. It acts only on the B component. The blend comprises two species – A and B – which interact via a square well potential of depth ϵ . The contact of like monomer in the range of the interaction $r \leq \sqrt{6}$ lowers the energy by an amount ϵ whereas the contact of unlike monomers increases the energy by ϵ . The energy scale of the mutual interactions sets the temperature scale.

In our model the thermal interactions can be related to the Flory–Huggins parameter via the intermolecular pair correlation function $g^{\text{inter}}(r)$. This quantity measures the probability of finding a monomer of another chain at a distance r . Clearly, only the interactions between different chains contribute to the energy of mixing, and we obtain:

$$\chi = \frac{2\epsilon}{k_B T} \int_{r \leq \sqrt{6}} d\mathbf{r}^3 g^{\text{inter}}(\mathbf{r}) \approx 5.3\epsilon \quad (1)$$

where the last expression holds for flexible chains. Entropic contributions are small compared to the enthalpic ones for the parameters considered in the following. A more detailed account of the thermodynamics of the homogenous system can be found in Ref⁴.

Unless noted otherwise we use chain length $N = 32$ in our simulations. This corresponds roughly to a degree of polymerization of 100-150. Two types of simulation schemes have been employed to investigate interfacial properties: simulations of the interface in the canonical ensemble and simulations in the semi-grandcanonical ensemble in junction with reweighting techniques. In the semi-grandcanonical ensemble the composition of the

mixture fluctuates and the chemical potential difference $\Delta\mu$ between the polymer species is held fixed. The Monte Carlo Scheme comprises two types of movements: Canonical moves which relax the conformations of the polymers on the lattice and switches of the chain identity $A \rightleftharpoons B$. In the latter scheme the Hamiltonian, which is simulated, is modified as to encourage the system to sample configurations which contain interfaces. In this way all excess quantities of the interface (e.g., interfacial tension, interfacial energy, or the enrichment of copolymers) are accurately measurable in the simulations. The canonical simulations can also take advantage of the fast relaxation of identity switches by exchanging the identity between pairs of polymers.

The Monte Carlo simulations are compared to self-consistent field (SCF) calculations. Either the Gaussian chain model is used (and the chain dimensions are identified via the end-to-end distance R_e as measured in the MC simulations), or the chain conformations are extracted from the simulation of a bulk system and the single chain partition function, required by the SCF scheme, is approximated by a large (more than 7×10^7) sample of single chain conformations. The latter scheme has advantages if the interfacial width becomes comparable to the persistence length of the polymer.

Results

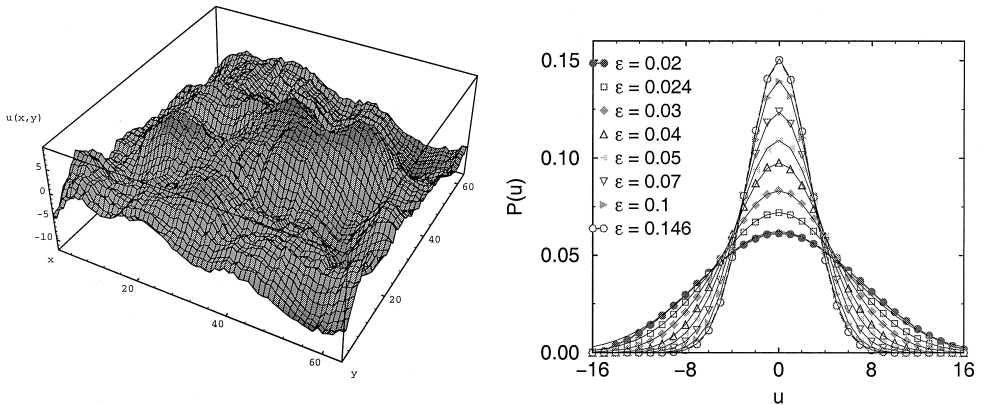


Figure 1: (a) Fluctuations of the local interface position in a binary polymer blend at $\epsilon = 0.03$ ($\chi N \approx 5.1$). The position has been averaged over a lateral size of $B = 8$. (b) Distribution of the local interface positions as a function of the incompatibility ϵ . From Werner *et al.*⁵⁾.

A comparison between simulations/experiments and SCF calculations has to take due account of the fluctuations of the local interface position. Interfaces are not perfectly flat, as assumed in the SCF calculations, but there are thermal fluctuations. A snapshot of the interface position in the MC simulations of a binary blend is shown in Fig.1(a). To a first approximation the effect of these fluctuations is to increase the effective area of the interface. Let $u(\mathbf{r}||)$ denote the local interface position. Then, the free energy cost of

deviations from perfectly flat configurations are described by the Hamiltonian \mathcal{H} :

$$\mathcal{H}[u(\mathbf{r}_{\parallel})] = \int d^2\mathbf{r}_{\parallel} \left\{ \frac{\sigma}{2} |\nabla u|^2 + \frac{\kappa}{2} |\Delta u|^2 \right\} \quad (2)$$

This is an expansion in terms of small u and its derivatives, σ denotes the interfacial tension and κ the bending rigidity. For interfaces between not too long homopolymers κ is very small; for copolymer laden interfaces, however, the second term becomes important as we shall discuss. This capillary wave Hamiltonian is diagonal and quadratic in terms of the Fourier components $u(q)$ and the equipartition theorem yields for the spectrum of fluctuations in thermal equilibrium:

$$\langle u^2(q) \rangle = \frac{k_B T}{\sigma q^2 + \kappa q^4} \quad (3)$$

The local positions $u(\mathbf{r}_{\parallel})$ are also Gaussian distributed $P(u)$ with variance s :

$$s^2 = \frac{1}{4\pi^2} \int d^2\mathbf{q}_{\parallel} \langle u^2(\mathbf{q}_{\parallel}) \rangle = \frac{k_B T}{2\pi\sigma} \ln \left(\frac{q_{\max}}{q_{\min}} \right) \quad (4)$$

where a short and long length scale cut-off q_{\max} and q_{\min} have to be introduced to avoid the divergence at $q \rightarrow 0$ and $q \rightarrow \infty$. The bending rigidity κ has been neglected, it would make the cut-off at small distance obsolete. The MC result for the distribution $P(u)$ of the local positions is presented in Fig.1(b). Upon decreasing the incompatibility ϵ , we increase the strength of the fluctuations.

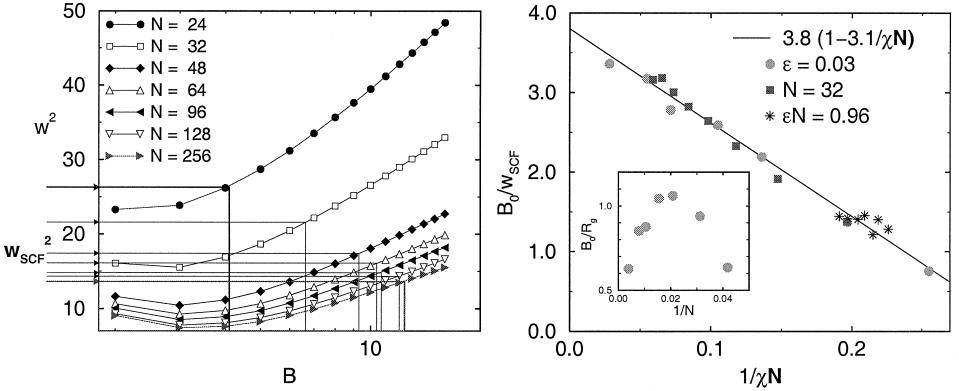


Figure 2: (a) Dependence of the apparent interfacial width on the lateral block size B at constant incompatibility $\epsilon = 0.03$ for different chain lengths. From the intersections of the simulation data with the self-consistent field predictions (presented as horizontal lines) we determine the small length scale cut-off B_0 . (b) The ratio B_0/w_{scf} approaches a constant value 3.8. Leading corrections are of the order $1/\chi N$. Note that data sets at constant N , χN and χ collapse in this representation. The inset shows the ratio B_0/R_e for fixed incompatibility $\epsilon = 0.03$. The ratio tends to zero for large N . From Werner *et al.*⁶⁾.

These capillary waves broaden the apparent profiles p_{app} . Laterally averaged profiles, as obtained in experiments or MC simulations, are describable via the convolution of an intrinsic profiles p_{int} of an ideally flat interfaces and the distribution of the local positions

$$p_{\text{app}}(z) = \int du P(u) p_{\text{int}}(z - u), \quad (5)$$

where z denotes the coordinate perpendicular. When applied to a erfc -shape profile, one obtains^{5,7}:

$$w_{\text{app}}^2 = w_{\text{int}}^2 + \frac{k_B T}{4\sigma} \ln \left(\frac{q_{\text{max}}}{q_{\text{min}}} \right) \quad (6)$$

The apparent width is broader than the intrinsic one and depends via the two cut-offs on the system geometry⁵. For a free interface the upper cut-off is set by the lateral block size B on which the interface is observed. This might be set by the size of the simulation cell or the coherence length of the neutron beam by which the interfacial structure is investigated. Gravitation or interactions with walls/surfaces also limit long wavelength fluctuations. On short distances the separation of fluctuation into “intrinsic” ones, which build up the smooth profile of the ideally flat interface, and capillary waves breaks down. Polymer blends are well suited to examine this crossover, because the strong interdigitation of the molecules makes self-consistent field calculations describe the properties of interfaces accurately except for capillary wave fluctuations. Taking the SCF prediction as the width of an hypothetical flat interface, we have used Eq.6 to determine the length scale $B_0 = 2\pi/q_{\text{max}}$ on which the crossover between the intrinsic fluctuations and capillary waves occurs. This procedure is illustrated in Fig.2(a). There are three possible candidates for B_0 : A microscopic length scale (e.g., the bond length) independent from temperature or chain length; the width of the interface, which depends on temperature but not on N ; or the radius of gyration/correlation length which depends both on χN and R_e . The simulation data⁶ in panel (b) indicate a behavior of the form $B_0 = 3.8w_{\text{scf}}(1 - 3.1/\chi N)$, i.e. the intrinsic width of the interface sets the crossover length; a result compatible with calculations of Semenov⁸.

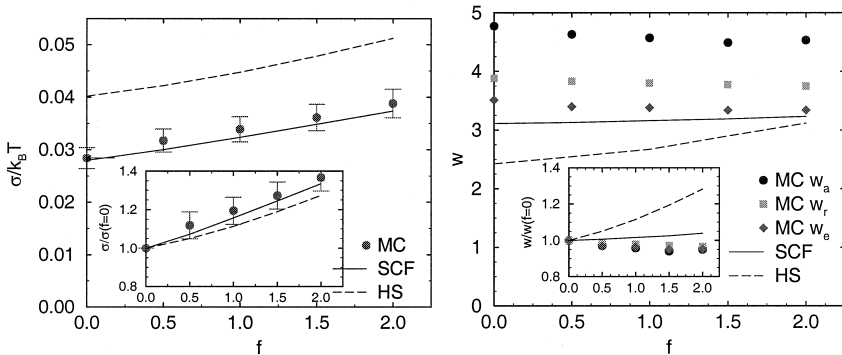


Figure 3: Interfacial tension (a) and interfacial width (b) in a blend of flexible ($f = 0$) and stiff (f as indicated) polymers at rather strong segregation $\epsilon = 0.05$. Comparisons with detailed SCF calculations, which take account of the chain architecture on all length scales, and predictions of the Gaussian chain model by Helfand and Sapse (HS) are shown. In panel (b) w_a denotes the apparent width, which is averaged over the whole lateral system size $L = 64$, w_r represents the width on the block size $B = 16$, and $w_e = 2\Delta e/\chi k_B T \rho$ denotes the width extracted from the excess energy Δe of the interface per unit area, respectively. From Müller and Werner⁶.

The spectrum of interfacial fluctuations is a route for measuring the interfacial tension in MC simulations. This is illustrated for a blend with a structural asymmetry in Fig.3. When we increase the stiffness disparity, the semi-grandcanonical identity switches be-

come increasingly inefficient and σ cannot be obtained via reweighting techniques. Upon increasing the stiffness, we increase the χ parameter (c.f. Eq.1), because the stiffer polymer has a more open structure and interacts with more neighboring monomers on different chains. Stiffness disparity gives also rise to an entropic contribution to χ , due to differences in the packing structure of the monomers⁴. For the rather large thermal interactions $\epsilon = 0.05$ this effect is, however, negligible. The increased incompatibility results in a larger interfacial tension (c.f. Fig.3(a)). This effect is quantitatively captured by the SCF calculations which account for the detailed chain architecture. Qualitative agreement is also obtained within the Gaussian chain model. The deviations from the prediction of Helfand and Sapse⁰ are mainly due to chain end corrections. The situation is qualitatively different for the intrinsic width of the interface (c.f. panel (b)). Monte Carlo simulations and SCF calculations predict no increase or even a reduction of the width for larger stiffness, while the intrinsic width increases in the Gaussian chain model. The break down of the Gaussian chain model can be qualitatively rationalized as follows: The width of the interface is determined by loops of the polymers into the other phase. For large incompatibility the width of the interface becomes comparable with the persistence length and the conformation of a loop differs from the Gaussian statistic of the chain on large length scales. Likewise, MC simulations, SCF calculations and predictions of the Gaussian chain model agree for smaller χ , where $w \gg b$.

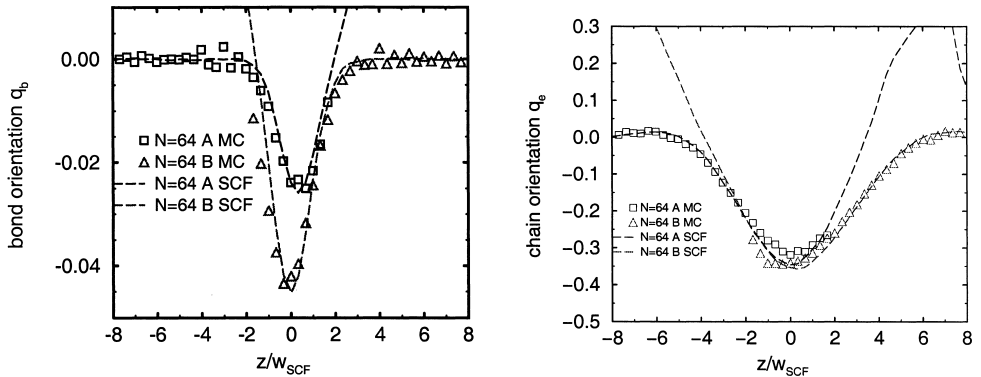


Figure 4: Orientations of the bond vector (a) and \vec{R}_e (b) in a blend of polymers with stiffness $f = 0$ (left side) and $f = 1$ (right side) at rather strong segregation $\epsilon = 0.05$ and chain length $N = 64$. Symbols denote the results of the MC simulation on a lateral length scale $B = 16$, while lines represent the SCF calculations. From Müller and Werner⁹.

The ability of the SCF calculations to provide a detailed description of the intrinsic interface structure is illustrated in Fig.4. We present the MC and SCF results for the orientations as measured by the 2nd Legendre polynomial of the angle between the bond vector or end-to-end distance \vec{R}_e with respect to the interface. Both vectors align parallel to the interface, but the effect is much stronger for \vec{R}_e and more stiffness dependent for the bond vectors.

Diblock copolymers are model surfactants for the AB homopolymer blend. They adsorb at the interface as to extend both halves into the corresponding homopolymer phases. This

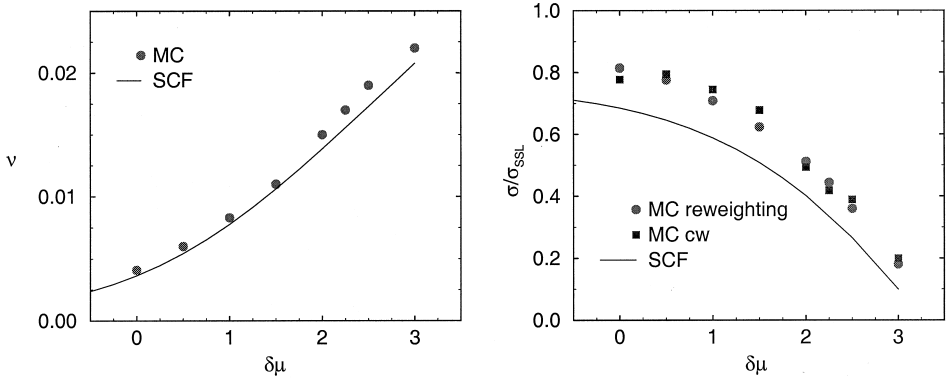


Figure 5: (a) Adsorption of diblock copolymers at a homopolymer/homopolymer interface as a function of the chemical potential of the copolymer at $\epsilon = 0.1$ and chain length $N = 32$. (b) Reduction of the interfacial tension upon adding copolymers. From Werner *et al.*¹¹⁾.

decreases their enthalpy, but the localization at the interface reduces the translational entropy and the conformational entropy due to chain stretching at high copolymer excess at the interface. Upon increasing the chemical potential $\delta\mu$ (or concentration) of the copolymers in the bulk, we observe the adsorption of copolymers at the interface and the concomitant reduction of the interfacial tension in Fig.5. Both MC simulations and SCF calculations agree at high segregation. However, rather than forming a dense copolymer brush at the interface, a phase separation into a homopolymer-rich phase and a lamellar phase (swollen by homopolymers) is encountered. For small ϵ the addition of copolymers

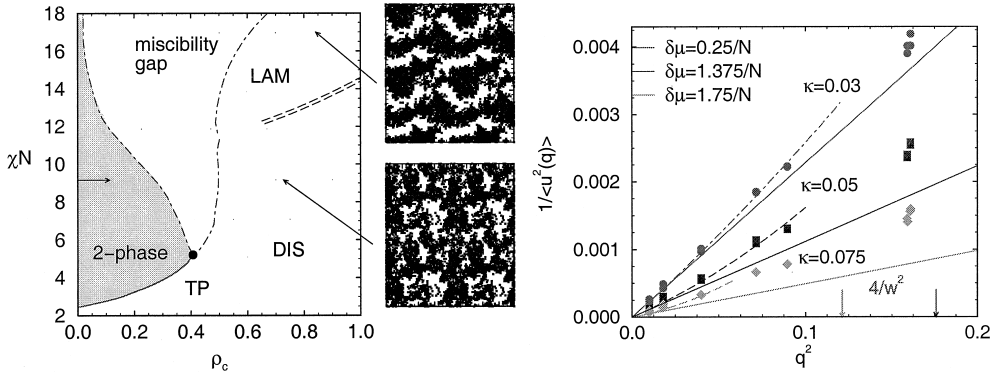


Figure 6: (a) Isopleth cut through the phase triangle of a ternary blend. (b) Spectrum of interface fluctuations in a ternary blend of two homopolymers and a diblock copolymer at $\epsilon = 0.054$. Estimates for the bending rigidity of the interfaces are indicated. From Müller and Schick¹²⁾.

drives the system to compatibility (c.f. Fig.6(a)). At intermediate segregation we find a three phase coexistence between two homopolymer-rich phases and a copolymer-rich disordered phase. The latter has a structure of a microemulsion (as revealed, e.g., by

the snapshots). SCF calculations by Janert and Schick¹³ rather predict highly swollen lamellar phases in this region. Some insight into this discrepancy can be gained from the spectrum of interface fluctuations. Upon adding copolymers to the systems at $\epsilon = 0.054$ we decrease the interfacial tension and deviations from a simple q^2 dependence become apparent (see panel (b)). We can obtain a rough estimate of the bending rigidity κ of the copolymer-loaden interface according to Eq.3. The bending rigidity turns out to be much smaller than $k_B T/2\pi$. It is this bending rigidity, however, which stabilizes the liquid-crystalline order of the lamellar phase. De Gennes and Taupin¹⁵ argued that a small value of κ leads to the formation of a microemulsion. Indeed this is observed in the simulation¹² and experiments¹⁴. If we were to increase the chain length we would increase the bending rigidity $\kappa \sim \sqrt{N}$ ¹⁶ and stabilize the lamellar phases predicted by the SCF theory.

Outlook

Interfaces in polymer blends have been investigated by simulations and the results have been compared to SCF calculations. Special attention has been focused on interface fluctuations. They broaden interfacial profiles, which are measured in experiments or simulations, and they lead to the formation of polymeric microemulsions. They are also important for the wetting behavior and the properties of confined systems⁷.

Acknowledgment: It is a pleasure to thank F. Schmid, A. Werner, and M. Schick for fruitful and enjoyable collaboration. Financial support from the DFG under grant Bi314/17 and access to the CRAY T3Es at the NIC Jülich, the HLR Stuttgart and the San Diego SC are acknowledged.

1. C. Creton, E.J. Kramer, and G. Hadzioannou, *Macromolecules* **24**, 1846 (1991)
2. G.I. Taylor, *Proc.R.Soc. London*, **A 138**, 41 (1932)
3. S.T. Milner, *MRS Bull.* **22**, 38 (1997)
4. M. Müller, *Macromol.Theory Simul.* **8**, 343 (1999)
5. A. Werner, F. Schmid, M. Müller, and K. Binder, *J.Chem.Phys.* **107**, 8175 (1997)
6. A. Werner, F. Schmid, M. Müller, and K. Binder, *Phys.Rev.* **E 59**, 728 (1999)
7. M.D. Lacasse, G.S. Grest, and A.J. Levine, *Phys.Rev.Lett.* **80**, 309 (1998)
8. A.N. Semenov, *Macromolecules* **27**, 2732 (1994)
9. M. Müller and A. Werner, *J.Chem.Phys.* **107**, 10764 (1997)
10. E. Helfand and A.M. Sapse, *J.Chem.Phys.* **62**, 1329 (1975)
11. A. Werner, F. Schmid, and M. Müller, *J.Chem.Phys.* **110**, 5370 (1999)
12. M. Müller and M. Schick, *J.Chem.Phys.* **105**, 885 (1996)
13. P.K. Janert and M. Schick, *Macromolecules* **30**, 3916 (1997)
14. G.H. Fredrickson and F.S. Bates, *Polym.Sci.* **B 35**, 2775 (1997)
H.S. Jeon, J.H. Lee, and N.P. Balsara, *Phys.Rev.Lett.* **79**, 3274 (1997)
15. P.G. de Gennes and C. Taupin *J.Phys.Chem.* **86**, 2294 (1982)
16. M.W. Matsen, *J.Chem.Phys.* **110**, 4658 (1999)
17. M. Müller and K. Binder, *Macromolecules* **31**, 8323 (1998)